Advances in Materials Research, *Vol. 14, No. 3 (2025) 185-203*
https://doi.org/10.12989/amr.2025.14.3.185

A study on transverse cracking in composite laminates subjected to flexural loading under asymmetrical environmental conditions

Mohamed Khodjet Kesba*[1], B. Boukert[1a], A. Benkhedda[1b] and E.A. Adda bedia[2c]

[1]*Aeronautical Sciences Laboratory, Institute of Aeronautics and Space Studies, University of Blida 1, BP 270 Route de Soumaa, Blida 09000, Algeria*
[2]*Laboratory of Materials and Hydrology, University of Sidi Bel Abbes, Sidi Bel Abbes, Algeria*

(*Received April 28, 2024, Revised April 20, 2025, Accepted April 21, 2025*)

Abstract. A present model was deployed to forecast the impact of transverse cracking on stiffness degradation in $[0/90]_{2s}$ composite laminates subjected to simple bending. Good alignment between the predictive model and empirical data from Smith and Ogin (2000) was achieved. The composite's material properties, influenced by temperature and moisture variations, are derived from a micromechanical laminate model. The transient and non-uniform moisture concentration distribution give rise to the transient elastic moduli of cracked composite laminates. This asymmetrical environment is considered in to evaluate changes in normalized axial and flexural modulus due to transverse cracking. The results adeptly depict the relationship between stiffness degradation and crack density, alongside operational temperature. Notably, composite laminates with transverse cracks undergoing simple bending exhibit less susceptibility to asymmetrical environment compared to those under tension loading. This theoretical study aims to enhance understanding of aged composite materials afflicted by matrix cracking.

Keywords: asymmetrical environment; bending; flexural stiffness; moisture concentration; transverse cracks

1. Introduction

In contrast to the extensive body of research on tensile loading (Li and Hafeez 2009, Vingradov and Hashin 2010, Barbero and Cosso 2014, Hajikazemi and Sadr 2014, Huang *et al*. 2014, Katerelos *et al*. 2015), there is a scarcity of literature focusing on the initiation of intralaminar matrix cracking in composite laminates under flexural loading. Early analytical efforts in understanding flexural behavior primarily revolved around developing beam theory for composite laminates and employing phenomenological failure criteria. However, these studies often had limited comparison with experimental data.

Khodjet Kesba *et al*. (2018) utilized a modified shear lag method to predict the impact of moisture absorption on stiffness degradation in $[0/90]_{2s}$ composite laminates with transverse cracks under

*Corresponding author, Ph.D., E-mail: mkhojet@gmail.com
[a] Ph.D., E-mail: bilanosky@hotmail.fr
[b] Professor., E-mail: aaminabenkhedda@gmail.com
[c] Professor., E-mail: addabed@yahoo.com

 ISSN: 2234-0912 (Print), 2234-179X (Online)

flexural loading. Good agreement was obtained by comparing the prediction model and experimental data published. The composite's material properties, influenced by temperature variation and moisture absorption, were considered. Transient and non-uniform distribution of moisture concentration contributed to transient elastic moduli in cracked composite laminates. By accounting for the hygrothermal effect, changes in normalized axial and flexural modulus due to transverse cracking were evaluated. The results effectively elucidate the dependency of stiffness degradation on crack density, moisture absorption, and operational temperature.

Zhihao *et al*. (2024) conducted an experimental investigation to examine the effects of various thermal cycling conditions on the mechanical behavior of carbon fiber/epoxy laminated composites. Three types of thermal cycling conditions involving continuous temperature variations were employed to assess the influence of temperature range on the residual tensile and in-plane shear moduli of the laminates. The test outcomes reveal that both the upper temperature limit and the temperature span of the thermal cycling conditions collectively impact the mechanical properties of CFRP composite laminates. Specifically, the residual tensile and in-plane shear moduli of the laminates decrease as the temperature span expands with a fixed upper limit. Conversely, when the temperature span remains constant, an increase in the upper temperature limit results in an elevation of the residual tensile modulus.

Chen *et al*. (2024) investigated the impact of temperature and moisture on the mechanical properties of carbon fiber composite materials. Tensile, compression, and shear tests were conducted on woven CFRP composites in four distinct composite environments: cold-temperature dry state, room-temperature dry state, elevated-temperature dry state, and elevated-temperature wet state. Fourier transform infrared spectroscopy was employed to analyze molecular composition and structure under these environmental conditions. Additionally, fracture morphology was analyzed to comprehend the deterioration mechanism of material properties at both macro and micro scales, the findings reveal that the tensile, compressive, and shear properties of the material decrease under harsh conditions, with the degradation effect on ultimate strength being notably greater than that on modulus. Composite environments significantly influence the macroscopic failure process and ultimate failure mode of materials. Overall, the temperature and humidity of the matrix system are central to the deterioration mechanism of composites, affecting the properties of the fiber/matrix interface and ultimately resulting in a loss of constitutive strength and bearing capacity.

Yuchi *et al*. (2024) delved into the mechanical degradation mechanism and statistical analysis of residual compressive strength in three lay-up laminates subjected to a seawater environment for over a year. The Fick and Langmuir models were employed to elucidate moisture absorption, while various characterization techniques were utilized to unveil the microstructural evolution of CFRP during aging, experimental findings revealed that the presence of multiple fiber directions creates additional channels for moisture absorption, resulting in a more pronounced wicking effect and a higher equilibrium moisture content, the choice of layup significantly influences the compression failure mode after prolonged aging, specifically the compressive strength of cross-ply and multidirectional laminates decreased by 50%, whereas that of unidirectional laminates decreased by 28%. Additionally, surface cracking was prominently observed in aged specimens, an empirical prediction model, grounded on the Langmuir model and experimental data, was proposed and validated using literature data.

Santosh *et al*. (2023) conducted a study to explore the influence of stacking sequence and thermal conditioning temperature on the flexural strength and interlaminar shear strength behavior of fiber-reinforced laminates. Laminates were fabricated using a hand-lay-up technique, with three different stacking sequences and three thermal conditioning temperatures selected for basalt fiber-reinforced

laminates. Thermal conditioning was carried out using a closed furnace at room temperature, 50˚C, and 80˚C for 2 hours, the results indicated that both the stacking sequence and thermal conditioning temperature significantly affected the flexural strength behavior of the laminates. Furthermore, investigation into the damage occurring on the fractured laminate specimen surfaces revealed that the stiffening of the resin matrix contributed to increased resistance and reduced deformability of the composite at room temperature. This effect may be attributed to the enhanced strength of the composite.

El Idrissi *et al*. (2023) introduced a novel progressive damage model aimed at accurately predicting the flexural behavior and damage evolution of composite laminates under three-point bending. This model considers both inter and intralaminar failure modes. It incorporates a progressive failure algorithm and gradual stiffness degradation rules through a user-defined subroutine to forecast further damage evolution post-damage initiation, one of the key objectives of this research was to develop a finite element model capable of simulating the behavior of various composite laminates under three-point bending, the results demonstrated significant agreement with experimental data, including degradation trends in load vs. deflection curves. The study also addressed the interaction between matrix cracking and delamination, as well as the impact of cohesive zone elements on material strength, it was discovered that interface strength plays a crucial role in fully utilizing laminate features and mitigating the effects of delamination, which can induce intra-laminar longitudinal cracks under higher inter-laminar stresses. This finding underscores the importance of considering interface strength in composite laminate design to enhance performance and durability.

Katarzyna and Falkowicz (2023) delved into the stability and failure analysis of thin-walled composite plate elements weakened by cut-outs and subjected to axial compression. The tested plates were constructed from carbon fiber reinforced polymer composite material. The research encompassed experimental tests on actual samples as well as numerical calculations utilizing the finite element method. Both experimental tests and numerical analyses were carried out across the entire loading spectrum until structural failure occurred, the numerical calculations were conducted through progressive failure analysis, which initiated failure according to Hashin's theory and further evolved based on an energy criterion. Numerical results depicting critical and post-critical states were compared with experimental research, revealing areas prone to material failure. The obtained findings showcased a high degree of agreement between the results of numerical analysis and experimental studies.

Hadj-djilani *et al*. (2023) conducted a study to explore the impact of hybridizing flax with Kevlar on the flexural and impact properties of Kevlar/flax/epoxy composites, employing three-point bending, drop-weight, and Charpy impact tests. The specimens were composed of unidirectional flax fibers (F) and woven Kevlar fibers (K) in four configurations: unidirectional flax/epoxy $[0_{16F}]$ (UFE), angle-ply flax/epoxy $[\pm 45_{4F}]_S$ (AFE), woven Kevlar/unidirectional flax/epoxy $[0–90_{2K}/0_{6F}]_S$ (UKFE), and woven Kevlar/angle-ply flax/epoxy $[0–90_{2K}/\pm 45_{3F}]_S$ (AKFE), results from the three-point bending test showcased a 15% increase in ultimate strength and flexural modulus for UKFE compared to pure UFE, and a more than threefold enhancement for AKFE compared to AFE laminates. Additionally, drop-weight test results revealed a notable 30% increase in impact force for both unidirectional and angle-ply laminate configurations. Charpy test outcomes indicated a remarkable 60% improvement in impact energies of the flax laminates, the predictions of the proposed finite element model closely aligned with the experimental results. These findings underscore the efficacy of hybridizing two layers of Kevlar onto flax/epoxy composites in bolstering their impact and flexural properties.

Qingping *et al*. (2021) conducted a comprehensive investigation into the failure mechanisms of open-hole cross-ply carbon fiber reinforced polymer (CFRP) laminated composites through a combination of experimental tests and computational modelling. Two effective methods were proposed: width-tapered double cantilever beam and fixed-ratio mixed-mode end load split tests, experimental results indicated that fracture energy was generally insensitive to crack length, eliminating the need for precise crack tip measurements. Comparisons between experimental results and failure surfaces predicted from curve fitting revealed good agreement between predictions and experimental data, the study systematically examined the failure mechanisms of open-hole cross-ply laminates under flexural loading using both experimental and multi-scale computational analyses. The initiation and propagation of delamination, as well as the failure of laminated layers, were comprehensively studied. Load-displacement curves predicted from computational analyses closely matched experimental observations. This integrated approach provided valuable insights into the behavior of open-hole cross-ply CFRP laminated composites under various loading conditions.

Some authors have investigated the behavior of carbon fiber reinforced polymer (CFRP) rectangular beam elements under flexural loading, as seen in studies such as those by Greif & Chapon (1993) and Echaabi *et al*. (1996). These studies often involved comparisons between experimentally observed loads at which first ply failure occurred and the predictions of engineering failure criteria. However, it was generally found that there was poor agreement between experimental observations and the predictions of these criteria.

Smith and Ogin (1999) introduced a one-dimensional model based on simple bending theory, which allows for the calculation of flexural stiffness as a function of crack density and provides predictions of first ply failure based on fracture mechanics principles. This model demonstrated good agreement with the flexural stiffness as a function of crack density in one of the 90/90 plies of a (0/90/90/0/90/90/0) lay-up, as observed in the approach by McCartney & Pierse (1997). A thermoelastic analysis was employed to derive an expression for residual curvature resulting from cracking, experimental data collected by Smith and Ogin (2000) encompassed crack onset and accumulation in the single 90° ply of a $(0/90)_{2s}$ glass fiber reinforced polymer (GFRP) laminate, correlating them with applied bending moment and in situ ply strain. Additionally, data on residual properties as a function of damage were obtained. The comparison between theoretical predictions and experimental results demonstrated satisfactory agreement.

In recent years, fiber-reinforced composite materials have experienced widespread utilization across various industries, including marine, automotive, and aerospace sectors. However, during operational life, environmental variations lead to a reduction in the elastic modulus of laminated materials, as evidenced by studies such as those by Shen and Springer (1981), Bowles (1989), and Upadhyay (2000), particular interest is the increasing attention towards polymer composite materials at high temperatures, primarily due to their suitability for critical aircraft components like transport airframe structures and aircraft engine parts. However, the matrix in polymer composite materials is highly susceptible to variations in moisture and temperature. Elevated temperatures coupled with high moisture concentration lead to increased matrix degradation, consequently diminishing the mechanical characteristics of composite laminates.

Numerous studies, including those by Tounsi *et al*. (2005), Amara *et al*. (2006, 2014), Benzair *et al*. (2006), Bouazza *et al*. (2007), Adda Bedia *et al*. (2008), Benkhedda *et al*. (2008), Rezoug *et al*. (2011), Bouderba *et al*. (2013), Zidi *et al*. (2014), Khodjet kesba *et al*. (2015), Chattibi *et al*. (2015), Khodjet kesba *et al*. (2016, 2018, 2019), have highlighted the significant degradation in mechanical properties of high-temperature composite materials under such conditions. Consequently, understanding the damage and failure mechanisms of these high-temperature composites is

imperative before their confident industrial use.

The present study is employed to predict the transverse cracking behavior in a symmetric cross-ply $[0/90]_{2s}$ laminate under flexural loading. The results obtained from this model exhibit favorable agreement when compared with experimental data (Smith and Ogin 2000), albeit without considering the temperature effect, the cross-ply laminates undergo hygrothermal aging initially and are subjected to transient and non-uniform moisture concentration distribution under asymmetrical environmental conditions. The results obtained from this analysis reveal the dependency of axial and flexural stiffness degradation on crack density and operational temperature.

2. Theoretical analysis

Transverse matrix cracking represents a prevalent form of damage in cross-ply laminates subjected to flexural loading. In this scenario, it is assumed that the 90° ply has developed continuous intralaminar cracks oriented in the fiber direction, extending from one edge to the other in the z direction. The cross-ply laminate is characterized by parameters: $2.t_{90}$, representing the width of the 90° ply, and $2.l_0$, indicating the spacing between two consecutive cracks (see Fig. 1).

The laminate is acted upon by a bending moment, M, which introduces a curvature radius R or curvature k (k =1/R). The longitudinal stress in each ply is given as a function of z coordinate by the following equation:

$$\sigma_{xx}(z) = \frac{E(z) \cdot z}{R} \tag{1}$$

Integrating through the laminate thickness, we derive a relationship between bending moment and curvature as follows:

$$\frac{M}{k} = \frac{wh^3}{12}\left(\frac{88E_0 + 40E_{90}}{128}\right) \tag{2}$$

where E_0 and E_{90} denote the 0° and 90° plies modulus in x-direction.

Eq. (2) may be rewritten as

$$\frac{M}{k} = \frac{wh^3}{12} E^0_{flex} \tag{3}$$

where E^0_{flex} is the initial flexural stiffness of the laminate derived using the simple bending theory, it's given by

$$E^0_{flex} = \left(\frac{88E_0 + 40E_{90}}{128}\right) \tag{4}$$

In absence of a unified theory for the mechanical characterization of composites materials with long fibers, various formulations have been proposed in the literature, we can quote, the mixtures rule method, the continuity method based on fibers arrangement (Staab 1999, Maurice 2001), the semi-empirical method based on Halpin-Tsai (Haplin and Tsai 1968) and the additional technique method based on fibers emplacement (Chamis 1984).

In this paper, we utilized the rule of mixtures method applied to composites with anisotropic fibers, which was modified by Hahn as described in Ref (Tsai, 1988). Therefore, the longitudinal Young's modulus for a unidirectional composite is given by:

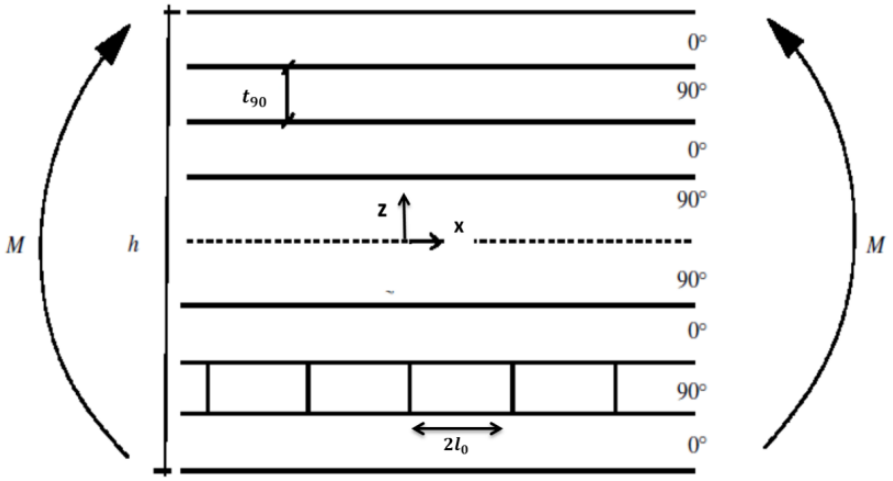

Fig. 1. Transverse cracked cross-ply laminate loaded in flexure

$$E_x = E_m \cdot V_m + E_{fx} \cdot V_f \tag{5}$$

The modified micromechanics method of transverse modulus for graphite/epoxy (T300/5208) composite is given by:

$$E_y = \frac{1 + 0.516\left(V_m/V_f\right)}{\frac{1}{E_{fy}} + \frac{0.516\left(V_m/V_f\right)}{E_m}} \tag{6}$$

In the same manner, we can obtain the shear modulus

$$G_{xy} = \frac{1 + 0.316\left(V_m/V_f\right)}{\frac{1}{G_{fx}} + \frac{0.316\left(V_m/V_f\right)}{G_m}} \tag{7}$$

$$\nu_{xy} = V_f \cdot \nu_f + V_m \cdot \nu_m \tag{8}$$

In the above equations, V_f and V_m are the fiber and matrix volume fractions, related by

$$V_f + V_m = 1 \tag{9}$$

E_f, G_f and ν_f are Young's modulus, shear modulus and Poisson's ratio, respectively, of fiber and E_m, G_m and ν_m are the corresponding properties of matrix.

To assign a stiffness value to any cracked 90° ply, we employ a one-dimensional modified shear-lag analysis for cross-ply laminate loaded in flexure. This approach assumes that the basic morphology of the cracks generated under flexural loading is similar to that of cracks resulting from tensile loading.

For that, when the applied loading is only in x-direction and the far field applied stress is defined by $\sigma_c = (1/2h)N_x$,where $\mathrm{N_x}$ is the applied load. The following analysis will be performed

assuming generalized plane strain condition:

$$\varepsilon_y^0 = \varepsilon_y^{90} = \varepsilon_y = const \tag{10}$$

The symbol ($\bar{}$) over stress and strain components denotes volume average. They are calculated using the following expressions:

- In the 0° layer: $\overline{f^0} = \frac{1}{2l_0}\frac{1}{t_0}\int_{-l_0}^{+l_0}\int_{t_{90}}^{h} f^0\, dxdz = \frac{1}{2\overline{l_0}}\frac{1}{\alpha}\int_{-\overline{l_0}}^{\overline{+l_0}}\int_{1}^{\overline{h}} f^0\,(\overline{x},\overline{z})d\overline{x}d\overline{z}$ (11)

- In the 90° layer: $\overline{f^{90}} = \frac{1}{2l_0}\frac{1}{t_{90}}\int_{-l_0}^{+l_0}\int_{0}^{t_{90}} f^{90}\, dxdz = \frac{1}{2\overline{l_0}}\frac{1}{\alpha}\int_{-\overline{l_0}}^{\overline{+l_0}}\int_{0}^{1} f^{90}\,(\overline{x},\overline{z})d\overline{x}d\overline{z}$ (12)

By utilizing the strain in the 0° layer, which remains undamaged and thus experiences laminate strains ($\varepsilon_x = \overline{\varepsilon}_x^0$, etc.) and assuming that the residual stresses are zero, the Young's modulus of the laminate with cracks may be defined by the following expression:

$$E_x = \frac{\sigma_c}{\overline{\varepsilon}_x^0} \tag{13}$$

Note that, the initial laminate modulus measured at the same load is $E_{x0} = \sigma_c/\varepsilon_{x0}$ and, hence

$$\frac{E_x}{E_{x0}} = \frac{\varepsilon_{x0}}{\overline{\varepsilon}_x^0} \tag{14}$$

Strain- stress equations are giving in the following form:

a) In the 0° layer: $$\begin{Bmatrix}\varepsilon_x^0\\ \varepsilon_y^0\\ \varepsilon_z^0\end{Bmatrix} = \begin{bmatrix}S_{11}S_{12}S_{13}\\ S_{12}S_{22}S_{23}\\ S_{13}S_{23}S_{33}\end{bmatrix}\begin{Bmatrix}\sigma_x^0\\ \sigma_y^0\\ \sigma_z^0\end{Bmatrix} \tag{15}$$

b) In the 90° layer: $$\begin{Bmatrix}\varepsilon_x^{90}\\ \varepsilon_y^{90}\\ \varepsilon_z^{90}\end{Bmatrix} = \begin{bmatrix}S_{22}S_{12}S_{23}\\ S_{12}S_{11}S_{12}\\ S_{23}S_{12}S_{22}\end{bmatrix}\begin{Bmatrix}\sigma_x^{90}\\ \sigma_y^{90}\\ \sigma_z^{90}\end{Bmatrix} \tag{16}$$

where S_{ij} is the compliance matrix for $[0/90]_{2s}$ composite laminate.

By averaging Eqs. (15) and (16), we obtain averaged constitutive equations of the 90° and 0° layer. In the averaged relationships we have $\overline{\sigma}_z^{90} = \overline{\sigma}_z^0 = 0$ which follows from the force equilibrium in z direction:

$$\int_{-l_0}^{+l_0} \sigma_z^i\, dx = 0, i = 90, \beta \tag{17}$$

Averaged constitutive equations corresponding to in-plane normal stress and strain components are

$$\begin{Bmatrix}\overline{\varepsilon_x^0}\\ \varepsilon_y\end{Bmatrix} = \begin{bmatrix}S_{11}\,S_{12}\\ S_{12}\,S_{22}\end{bmatrix}\begin{Bmatrix}\overline{\sigma_x^0}\\ \overline{\sigma_y^0}\end{Bmatrix} \tag{18}$$

$$\begin{Bmatrix} \overline{\varepsilon_x^{90}} \\ \varepsilon_y \end{Bmatrix} = \begin{bmatrix} S_{22}\, S_{12} \\ S_{12}\, S_{11} \end{bmatrix} \begin{Bmatrix} \overline{\sigma_x^{90}} \\ \overline{\sigma_y^{90}} \end{Bmatrix} \tag{19}$$

Eqs. (18) and (19) are derived from the 3D strain-stress relationships. However, due to Eq. (17), the result is similar to classical thin-laminate theory (CLT). In fact, for an undamaged laminate, the averaged stresses and strains are equivalent to the laminate theory stresses and strains, and Eqs. (18) and (19) remain applicable.

Force equilibrium equations for a damaged (or undamaged) laminate are:

- In x-direction: $N_x = \int_0^{t_{90}} \sigma_x^{90}\, dz + \int_{t_{90}}^{h} \sigma_x^0\, dz = \sigma_c(t_{90} + t_0)$ (20)

  Leading to $\overline{\sigma_x^{90}} t_{90} + \overline{\sigma_x^0} t_0 = \sigma_c(t_{90} + t_0)$ (21)

- In y-direction: $N_y = 0 \Rightarrow \int_0^{t_{90}} \sigma_y^{90}\, dz + \int_{t_{90}}^{h} \sigma_x^0\, dz = 0$ (22)

  From which follows $\overline{\sigma_y^{90}} t_{90} + \overline{\sigma_y^0} t_0 = 0$ (23)

Eqs. (18), (19), (21), and (23) involve seven unknowns: four stress components and three strain components ($\bar{\varepsilon}_x^{90}$, $\bar{\varepsilon}_x^0$ and ε_y). However, the total number of equations is six. Therefore, one of the unknowns can be considered as independent, and the rest can be expressed as linear functions of it. By selecting the stress $\bar{\sigma}_x^{90}$ as the independent variable and solving the system of equations (18), (19), (21), and (23) with respect to it, we obtain:

$$\varepsilon_y = g_1 \overline{\sigma_x^{90}} + f_1 \sigma_c; \qquad \overline{\varepsilon_x^{90}} = g_2 \overline{\sigma_x^{90}} + f_2 \sigma_c; \overline{\varepsilon_x^0} = g_3 \overline{\sigma_x^{90}} + f_3 \sigma_c \tag{24}$$

Expressions for g_i, f_i , i=1,2,3 through laminate geometry and properties of constituents are given as follows

$$g_1 = t_{90} \frac{S_{12}S_{22} - S_{11}S_{12}}{S_{11}t_0 + S_{22}t_{90}} \quad ; \quad f_1 = \frac{S_{11}S_{12}(t_0 + t_{90})}{S_{11}t_0 + S_{22}t_{90}} \tag{25}$$

$$g_2 = S_{22} - \frac{S_{12}(S_{12}t_0 + S_{12}t_{90})}{S_{11}t_0 + S_{22}t_{90}} \quad ; \quad f_2 = \frac{S_{12}S_{xy}^0(t_0 + t_{90})}{S_{11}t_0 + S_{22}t_{90}} \tag{26}$$

$$g_3 = \frac{t_{90}}{t_0}\left(S_{12} \frac{(S_{12}t_0 + S_{12}t_{90})}{S_{11}t_0 + S_{22}t_{90}}\right) - S_{11} \quad ; \quad f_3 = \frac{t_0 + t_{90}}{t_0}\left(S_{11} - \frac{(S_{12})^2 t_{90}}{S_{11}t_0 + S_{22}t_{90}}\right) \tag{27}$$

To derive an expression for the average stress $\bar{\sigma}_x^{90}$ in the repeatable unit, we examine the axial stress perturbation induced by the presence of two cracks. Without loss of generality, the axial stress distribution can be expressed in the following form:

$$\sigma_x^{90} = \sigma_{x0}^{90} - \sigma_{x0}^{90} f_1(\overline{x}, \overline{z}) \tag{28}$$

$$\sigma_x^0 = \sigma_{x0}^0 - \sigma_{x0}^{90} f_2(\overline{x}, \overline{z}) \tag{29}$$

where σ_{x0}^{90} is the CLT stress in 90° layer and σ_{x0}^0 is CLT stress in the 0° layer (laminate theory routine), $-\sigma_{x0}^{90} f_1(\bar{x}, \bar{z})$ and $\sigma_{x0}^{90} f_2(\bar{x}, \bar{z})$ are stress perturbation caused by crack. Normalizing factors form of far field stresses in perturbation functions are used for convenience. Averaging Eqs. (28) and (29) using the integral force equilibrium in x-direction (Eq. (20)), we obtain

$$\overline{\sigma_x^{90}} = \sigma_{x0}^{90} - \sigma_{x0}^{90}\frac{1}{2\overline{l_0}}R(\overline{l_0}) \tag{30}$$

$$\overline{\sigma_x^{\beta}} = \sigma_{x0}^{\beta} - \sigma_{x0}^{90}\frac{1}{2\alpha\overline{l_0}}R(\overline{l_0}) \tag{31}$$

In the following function:

$$R(\overline{l_0}) = \int_{-\overline{l_0}}^{\overline{l_0}}\int_0^1 f_1(\overline{x},\overline{z})d\overline{z}d\overline{x} \tag{32}$$

$R(\overline{l_0})$ is called the stress perturbation function. It's related to axial stress perturbation in the 90° layer and depends on the crack density.

The average stress $\overline{\sigma}_x^{90}$ involved in Eq. (24) is now expressed through the stress perturbation function (Eq. (32)). Conditions used to obtain expressions (Eq. (24)) are the same as used in CLT. Hence, substituting $\overline{\sigma}_x^{90} = \sigma_{x0}^{90}$ where σ_{x0}^{90} is the x-axis stress in the 90° layer according to CLT, we obtain CLT solution: $\overline{\varepsilon}_x^{90} = \varepsilon_{x0}^{90} = \varepsilon_{x0}$,$\overline{\varepsilon}_x^{0} = \varepsilon_{x0}^{0} = \varepsilon_{x0}$ and $\varepsilon_y = \varepsilon_{y0}$.

Substituting Eq. (30), which contains two terms, in Eq. (24) the result has two terms. The first term according to the discussion above is equal to CLT strain but the second one is a new term related to the stress perturbation function $R(\overline{l_0})$:

$$\varepsilon_y = \varepsilon_{y0} - \sigma_{x0}^{90} g_1 \frac{1}{2\overline{l0}}R(\overline{l0}) \tag{33}$$

$$\overline{\varepsilon_x^{90}} = \varepsilon_{x0} - \sigma_{x0}^{90} g_2 \frac{1}{2\overline{l0}}R(\overline{l0}) \tag{34}$$

$$\overline{\varepsilon_x^{0}} = \varepsilon_{x0} - \sigma_{x0}^{90} g_3 \frac{1}{2\overline{l0}}R(\overline{l0}) \tag{35}$$

The stress σ_{x0}^{90} in the 90° layer of an undamaged laminate under mechanical loading may be calculated using CLT:

$$\sigma_{x0}^{90} = Q_{22}\varepsilon_{x0}(1 - \nu_{12}\nu_{xy}^{0}) \tag{36}$$

Here, v_{xy}^{0} is the Poisson's ratio of the undamaged laminate.

2.1 Flexural stiffness as a function of crack density

When the 90° layer towards the tensile face of the laminate undergoes matrix cracking, the effective modulus of the ply is reduced from E_{90} to E_{90}^{*}. The value of E_{90}^{*} can be estimated using a modified shear-lag analysis of a representative cross-ply laminate of $[0/90]_s$ lay-up. If we write the reduced modulus as:

$$E_{x0} = \frac{t_0 E_0 + t_{90} E_{90}^{*}}{h} \tag{37}$$

where,

Table 1 Material properties of GFRP laminate used in calculations (Smith and Ogin 2000)

Proprieties Material	E_L (GPa)	E_T (GPa)	G_{LT} (GPa)	$G_{TT'}$ (GPa)	υ_{LT}	V_f
GFRP	37	9.5	4	3.345	0.28	0.52

$$E_{90}^{*} = \frac{E_{90}\left(1 - \frac{tanh(\xi\overline{l_0})}{\xi\overline{l_0}}\right)}{\left(1 + \frac{t_{90}E_{90}}{t_0E_0}\frac{tanh(\xi\overline{l_0})}{\xi\overline{l_0}}\right)} \tag{38}$$

The reduced flexural stiffness of the laminate can now be derived using the method detailed in Smith & Ogin (1999). Initially, it's noted that due to the reduced stiffness of the 90° ply, the neutral axis of the laminate will shift towards the compression face of the beam. Assuming that the distance moved δ_{NA} is sufficiently small that the neutral axis remains within the central 90°/90° layer, it can be shown that δ_{NA} is given by:

$$\delta_{NA} = \frac{5(E_{90} - E_{90}^{*})t_{90}}{8E_0 + 2E_{90}^{*} + 6E_{90}} \tag{39}$$

The reduced flexural stiffness can then be found as (Smith and Ogin 2000):

$$\frac{E_{flex}}{E_{flex}^{0}} = \frac{2(88E_0 + 21E_{90} + 19E_{90}^{*}) - \left(\frac{75(E_{90} - E_{90}^{*})^2}{8E_0 + 2E_{90}^{*} + 6E_{90}}\right)}{2(88E_0 + 40E_{90})} \tag{40}$$

Which may be approximated at large crack spacing as:

$$\frac{E_{flex}}{E_{flex}^{0}} = 1 - \frac{19E_{90}}{88E_0 + 40E_{90}}\left(1 + \frac{t_{90}E_{90}}{t_0E_0}\right)\frac{2}{\xi}\left(\frac{1}{2\rho}\right) \tag{41}$$

3. Materials and method

A computer code based on the preceding equations was developed to compute the degradation of stiffness properties.

3.1 Comparison of predictions with experimental data

In this section, we will validate the results of the present program without considering the hygrothermal effect on the material properties. The obtained results will be compared with experimental data for a GFRP laminate (Smith and Ogin 2000). The material properties of the selected composite are summarized in Table 1.

The degradation of flexural stiffness with respect to transverse crack density for $[0/90]_{2s}$ GFRP laminate loaded in bending and tension, respectively, is illustrated in Fig. 2. The largest measured reductions in flexural stiffness generally fell within the range of 2-4% (Fig. 2). These reductions are

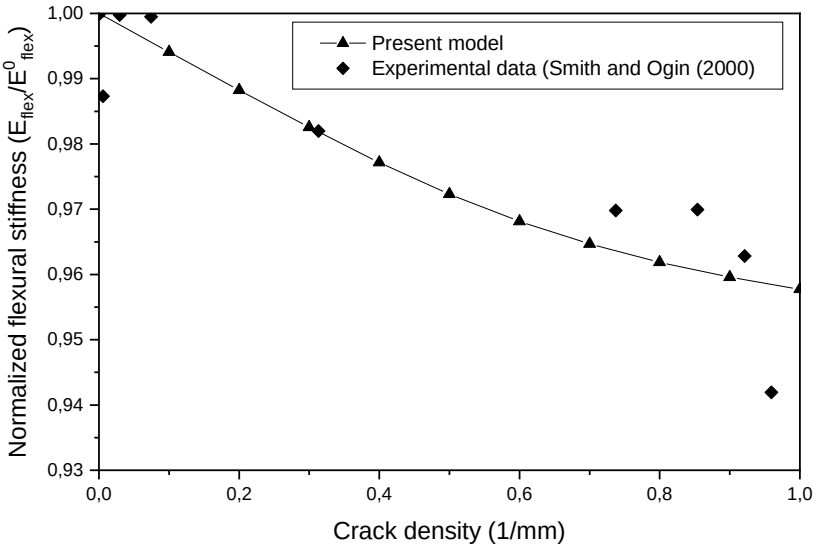

Fig. 2 The normalised flexural stiffness of $[0/90]_{2s}$ GFRP laminate loaded in flexure as a function of crack density

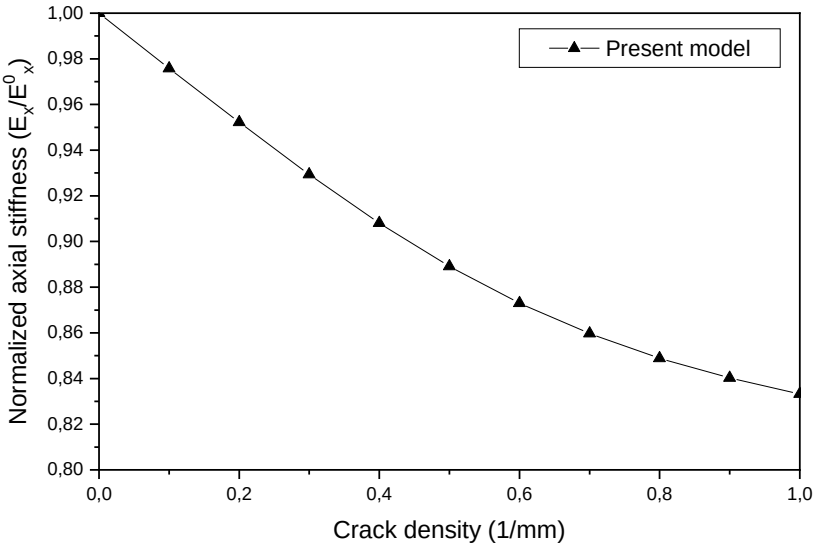

Fig. 3 The normalised axial stiffness of $[0/90]_{2s}$ GFRP laminate loaded in tension as a function of crack density

notably lower compared to similar lay-ups loaded in tension, where the axial stiffness reduction ranges from about 15 to 20% (Fig. 3). The relatively smaller reduction in flexural stiffness is attributed to only 25% of the available 90° plies cracking under load, as well as the greater influence of the 0° plies in determining the flexural modulus of the laminates as opposed to tensile modulus, Fig. 2 depicts the predictions made by the modified shear-lag model alongside the experimental data reported by Smith and Ogin (2000). Good agreement is achieved between the predicted model and the experimental data.

Table 2 Fiber and matrix characteristics of graphite/epoxy (T300/5208) (Tsai 1988) (T=22°C and C=0.5%)

E_{fx}^0 (Gpa)	E_{fx}^0 (Gpa)	E_m^0 (Gpa)	ν_{fx}^0	ν_m^0	G_{fx}^0(Gpa)	G_m^0(Gpa)	V_f
259	18.69	3.4	0.25	0.35	19.69	1.26	0.7

Table 3 Parameters of temperature and moisture characteristics variation (Tsai 1988)

T_g^0 (°C)	T_{room} (°C)	g (°C/c)	a	f
160	22	2000	0.35	0.04

3.2 Influence of asymetrical environment on flexural stiffness modulus

This study focuses on the reduction of axial and flexural stiffness properties due to transverse cracking in $[0/90]_{2s}$ composite laminate exposed to various environmental conditions. The model employed to incorporate aging and observe its impact on both fiber and matrix scales is the Tsai model (1988). This simplified method operates on the principle of considering the actual distribution of moisture concentration through each ply by employing its serial expansion (Vergnaud, 1992). Subsequently, it determines the precise expression of the normalized stiffness under the influence of hygrothermal effects.

$$T^* = \frac{T_g - T_{opr}}{T_g - T_{rm}} \tag{42}$$

where T_g represents the glass transition temperature, T_{opr} denotes the operating temperature, and T_{rm} represents the room temperature. Additionally, we make the assumption that moisture suppresses the glass transition temperature T_g^0 by a simple temperature shift.

$$T_g = T_g^0 - g \cdot c \tag{43}$$

Here, T_g^0 represents the glass transition temperature at the dry state, g denotes the temperature shift per unit moisture absorbed, and c signifies the moisture absorbed. We can utilize the exponents of T^* to empirically fit the matrix of the mechanical properties as a function of moisture and temperature.

$$\frac{E_m}{E_m^0} = \frac{G_m}{G_m^0} = \frac{\nu_m}{\nu_m^0} = (T^*)^a \tag{44}$$

E_m^0, G_m^0 , ν_m^0 and represent the Young's modulus, shear modulus, and Poisson's ratio, respectively, of the matrix at room temperature, and a is the empirical constant. The same exponents of T^* are utilized to empirically fit the fiber mechanical properties as a function of moisture and temperature.

$$\frac{E_{fx}}{E_{fx}^0} = \frac{E_{fy}}{E_{fy}^0} = \frac{G_{fx}}{G_{fx}^0} = \frac{\nu_{fx}}{\nu_{fx}^0} = (T^*)^f \tag{45}$$

E_{fx}^0, E_{fy}^0, G_{fx}^0 and ν_{fx}^0 are the longitudinal and transversal Young's modulus, shear modulus and Poisson's ratio, respectively, of the fibre at room temperature and f is the empirical constant.

It is assumed that E_m, G_m, ν_m, E_{fx}^0, E_{fy}^0, G_{fx}^0 and ν_{fx}^0 are function of temperature and moisture

Table 4 Moisture diffusion characteristics of graphite/epoxy (T300/5208) (Tsai 1988)

Diffusivity, mm^2/s	$D_z = 132\exp(-6750/T)$ T: Temperature (K)
Moisture concentration at the surface as a function of relative humidity, %	$C_1 = 0.015 \cdot HR_1, HR_1 = 100\%$ $C_2 = 0.015 \cdot HR_2, HR_1 = 50\%$ H: Relative humidity (%)

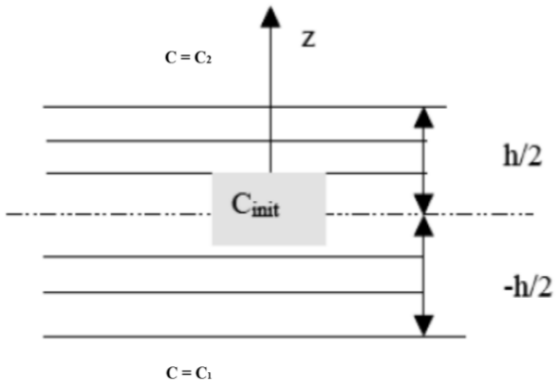

Fig. 4 The one-dimensional problem of asymmetrical environment diffusion in plates

(as described in Eqs. (44) and (45)), then E_x, E_y and G_{xy}(as described in Eqs. (5), (6) and (7)) will be also function of temperature and moisture. In Tables 2 and 3, we can find the data that influences mechanical characteristics of graphite/epoxy material.

Let's consider a laminated plate of thickness h made of polymer matrix composite, with both sides subjected to different dry environments. The plate is assumed to be infinite in both x and y directions, with moisture variation occurring only in the z direction (refer to Fig. 4). Consequently, the problem is one-dimensional. The lower side of the plate has a moisture concentration C_1 and a temperature T, the upper side has a concentration C_2 and a temperature T, the moisture concentration within the plate is governed by the Fick equation (Shen and Springer 1981, Tounsi *et al*. 2005, Benkhedda *et al*. 2008) with a diffusivity D_z.

$$\frac{\partial C}{\partial t} = D_z \frac{\partial^2 C}{\partial z^2} \tag{46}$$

With

$$C = C(z,t) \quad \text{at} \quad t = 0 \quad \text{for} \quad 0 < z < h \tag{47}$$

$$\begin{aligned} C = C_2 \quad &\text{at} \quad t > 0 \quad \text{for} \quad z = h \\ C = C1 \ &\text{at} \ t > 0 \ \text{for} \quad z = 0 \end{aligned} \tag{48}$$

The moisture diffusion characteristics are given in Table 4.

The initial conditions being uniform and the boundary conditions are constants, the unidimensional solution of Fick equation for asymmetrical environment can be expressed as (Tsai 1988, Sereir 2006):

$$C(z_k,t)=\left[C_1+(C_2-C_1)\frac{z_k}{h}+\frac{2}{\pi}\sum_{n=1}^{\infty}\frac{C2\,cos(n\pi)-C1}{n}\times sin\left(\frac{n\pi z_k}{h}\right)exp\left(\frac{-D_z n^2\pi^2 t}{h^2}\right)\right] \quad (49)$$

Very often, the laminated composite plate is symmetrical about the central plane (Fig. 4), and for the concentration's formulations are the most convenient if we take the surfaces at $z=\pm h/2$.

When z_k is replaced by $z_k \pm h/2$:

$$\begin{gathered} C = C_2 \quad \text{at} \quad t > 0 \quad \text{for} \quad z=+\frac{h}{2} \\ C = C1 \text{ at } t > 0 \text{ for } z=-\frac{h}{2} \end{gathered} \quad (50)$$

3.2.1 Relative flexural stiffness reduction analysis

Time t being given, the first step is to compute the on-axis free expansions E_x, E_y, G_{xy} and υ_{xy}. These expansions are computed at each point z_k of the thickness. Finally, the normalized axial and flexural stiffness degradation in $[0/90]_{2s}$ composite laminate as a function of crack density are evaluated and compared to the initial axial and flexural stiffness of the same uncracked laminate under the same environmental conditions. It should be noted that this initial stiffness of the uncracked laminate is a function of temperature and moisture distribution. Consequently, Eq. (41) becomes:

$$\frac{E_{flex(i)}}{E^0_{flex(i)}}=\frac{2(88E_{0(i)}+21E_{90(i)}+19E^*_{90(i)})-\left(\frac{75(E_{90(i)}-E^*_{90(i)})^2}{8E_{0(i)}+2E^*_{90(i)}+6E_{90(i)}}\right)}{2(88E_{0(i)}+40E_{90(i)})} \quad (51)$$

The index (i) represents the considered case of environmental conditions.

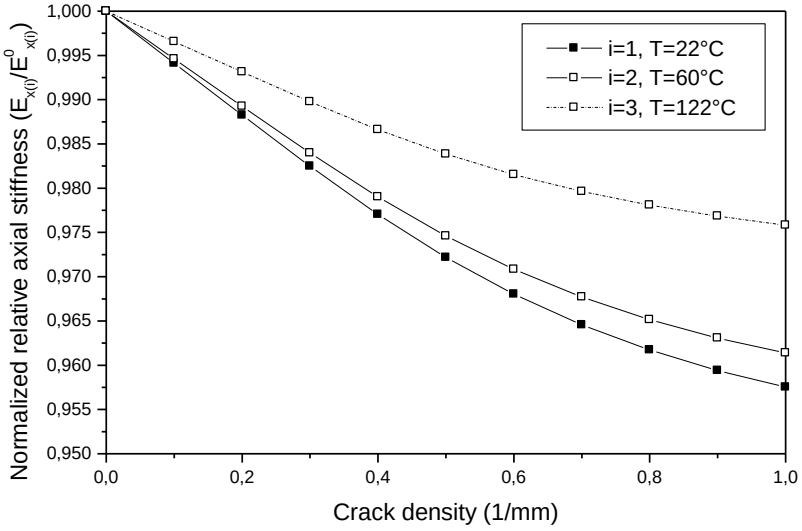

Fig. 5 Relative axial stiffness reduction as a function of crack density for a $[0/90]_{2s}$ graphite/epoxy (T300/5208) laminate

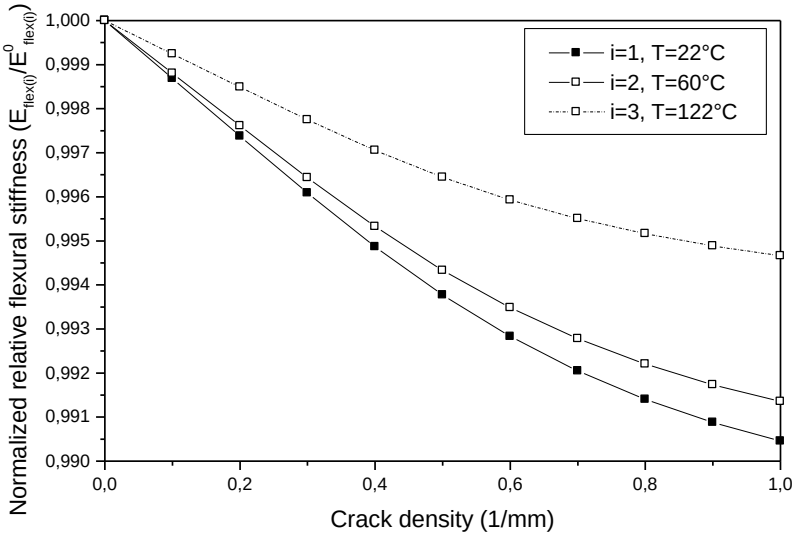

Fig. 6 Relative flexural stiffness reduction as a function of crack density for a $[0/90]_{2s}$ graphite/epoxy (T300/5208) laminate

The normalized axial and flexural stiffness degradation are depicted in a cross-ply $[0/90]_{2s}$ cracked laminate exposed to hygrothermal conditions, featuring a parabolic variation of longitudinal displacement in both 0° and 90° layers (where transverse cracks are located in the 90° layers). Transient and non-uniform moisture concentration have been chosen to represent the effect of high temperature in cracked composite laminates with asymmetrical environmental conditions.

In Figs. 5 and 6, the relative axial and flexural stiffness are plotted as a function of crack density with different values of operating temperatures. It is observed that both the axial and flexural modulus decrease monotonically with an increase in crack density and also with a decrease in temperature. The axial stiffness degradation shows a reduction of nearly 2% with a temperature decrease from 122°C to 22°C, compared to less than 0.5% reduction in flexural stiffness under the same conditions. This indicates that the composite laminate under bending load is less affected by the hygrothermal condition than the one under tension loading.

3.2.2 Total flexural stiffness reduction analysis

In this section, the total reduction of axial and flexural stiffness modulus is determined compared to the axial and flexural modulus of an uncracked laminate when the latter is initially exposed to case 1 of environmental conditions. Consequently, this total reduction of axial and flexural stiffness takes into account the reduction due to crack density and variation of moisture and temperature. Eq. (41) becomes:

$$\frac{E_{flex(i)}}{E^0_{flex(i)}} = \frac{\left(2(88E_{0(i)} + 21E_{90(i)} + 19E^*_{90(i)}) - \left(\frac{75(E_{90(i)} - E^*_{90(i)})^2}{8E_{0(i)} + 2E^*_{90(i)} + 6E_{90(i)}}\right)\right)(88E_{0(i)} + 40E_{90(i)})}{2(88E_{0(i)} + 40E_{90(i)})(88E_{0(1)} + 40E_{90(1)})} \quad (52)$$

In Figs. 7 and 8, the total axial and flexural stiffness are plotted as a function of crack density with different values of operating temperatures. It is observed that the total axial and flexural

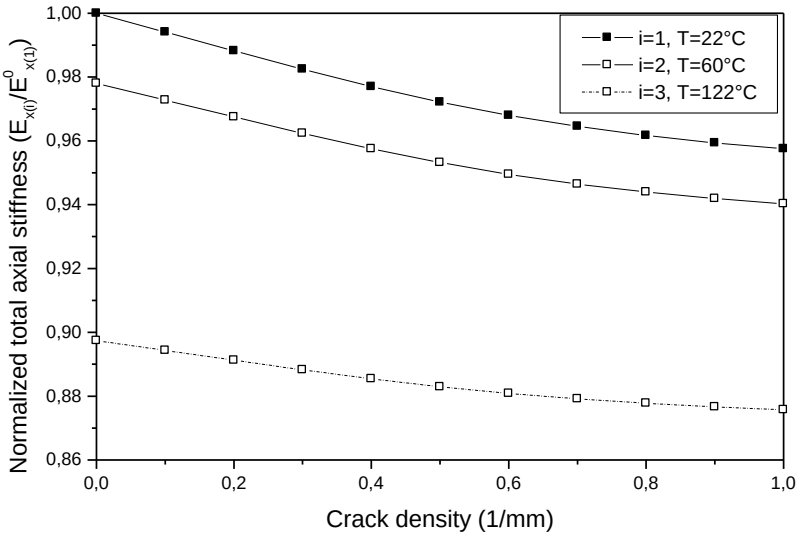

Fig. 7 Total axial stiffness reduction as a function of crack density for a $[0/90]_{2s}$ graphite/epoxy (T300/5208) laminate

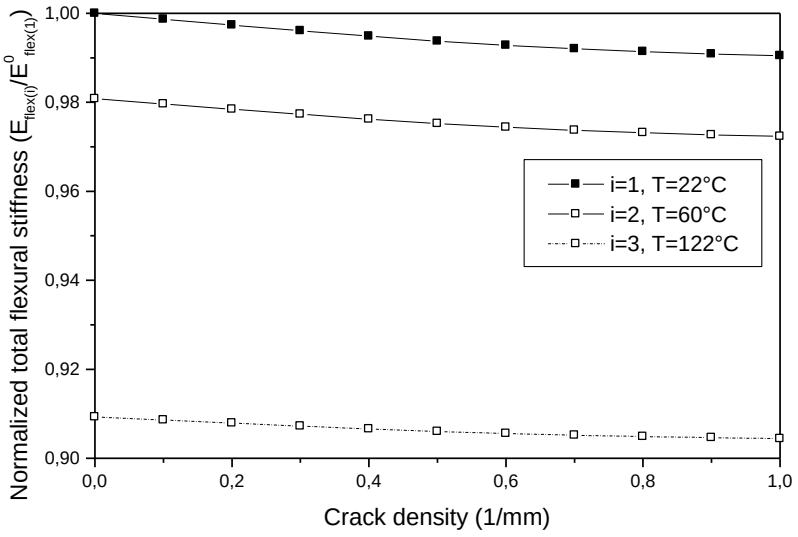

Fig. 8. Total flexural stiffness reduction as a function of crack density for a $[0/90]_{2s}$ graphite/epoxy (T300/5208) laminate

modulus decrease monotonically with increasing operating temperature and crack density. By analyzing the hygrothermal effect of a cracked laminate under different temperatures compared to an uncracked laminate under standard conditions (case 1: T=22°C and HR=0%), we note that the highest degradation of stiffness occurs at zero crack density. This indicates that the hygrothermal effect has a greater impact on the axial and flexural stiffness degradation for uncracked composite laminates than for those with transverse cracks.

4. Conclusions

The normalized flexural stiffness reduction was predicted using the present model for cross-ply composite laminates $[0/90]_{2s}$ with transverse cracks and under flexural load. A comparison of experimental and theoretical results showed satisfactory qualitative and quantitative agreement. The material properties are considered to be dependent on temperature and moisture, explicitly expressed in terms of fiber / matrix volume ratio and properties. The analysis has been extended to study the flexural stiffness properties degradation of high-temperature polymer composite material. Based on the present results, the following conclusions can be drawn:

• The axial and flexural stiffness degradation of the $[0/90]_{2s}$ composite laminates largely depend on the rise in crack density.

• The relative axial and flexural modulus reduce monotonically with increased crack density and with a decrease in operational temperature.

• The total axial and flexural modulus reduce monotonically with an increase in temperature and crack density.

• The composite laminate with transverse crack and under bending load is less affected by hygrothermal conditions than the one under tension loading.

• The asymmetrical environment has a greater impact on the axial and flexural stiffness degradation for an uncracked composite laminate than one with a transverse crack.

References

Adda bedia, E.A., Bouazza, M., Tounsi, A., Benzair, A. and Maachou, M. (2008), "Prediction of stiffness degradation in hygrothermal aged $[\theta_m/90_n]_s$ composite laminates with transverse cracking", *J. Mater. Proc.*, **199**, 199-205. https://doi.org/10.1016/j.jmatprotec.2007.08.002

Amara, K.H., Tounsi, A., Megueni, A. and Addabedia, E.A. (2006), "Effect of transverse cracks on the mechanical properties of angle-ply composite laminates", *Theor. Appl. Fract. Mech.*, **45**, 72-78. https://doi.org/10.1016/j.tafmec.2005.11.003

Amara, K.H., Bouazza, M., Antar, K. and Megueni, A. (2014), "Evaluation of the stiffness of composite materials with hygrothermal conditions", *Leona. J. Sci.*, **25**, 57-64.

Barbero, E.J., Cosso, F.A. (2014), "Determination of material parameters for discrete damage mechanics analysis of carbon-epoxy laminates", *Compos. Part B*, **56**, 638-646. https://doi.org/10.1016/j.compositesb.2013.08.084

Benkhedda, A., Tounsi A. and Addabedia, E.A. (2008), "Effect of temperature and humidity on transient hygrothermal stress during moisture desorption in laminated composite plates", *Compos. Struct.*, **82**, 629-635. https://doi.org/10.1016/j.compstruct.2007.04.013

Benzair, A., Maachou, M., Amara, K.H. and Tounsi, A. (2006), "Effect of transverse cracks on the elastic properties of high temperature angle-ply laminated composites", *Compos. Mater. Sci.*, **37**, 470-475. https://doi.org/10.1016/j.commatsci.2005.11.006

Berthelot, J.M., Leblonb, P., El Mahi A. and Le Core, J.F. (1996), "Transverse cracking of cross-ply laminated: Part Analysis", *Compos. Part A.*, **27**A, 989-1001. https://doi.org/10.1016/1359-835X(96)80002-A

Bouazza, M., Tounsi, A., Benzair, A. and Adda-bedia, E.A. (2007), "Effect of transverse cracking on stiffness reduction of hygrothermal aged cross-ply laminates", *Mater. Des.*, **28**(0), 1116-1123. https://doi.org/10.1016/j.matdes.2006.02.003

Bouderba B., Bouderba, M., Sid Ahmed H. and Tounsi A. (2013), "Thermomechanical bending response of FGM thick plates resting on Winkler–Pasternak elastic foundations", *Steel Compos. Struct.*, **14**(1), 85-104.

https://doi.org/10.12989/scs.2013.14.1.085
Bowles, D.E. and Tompkins, S.S. (1989), "Prediction of coefficients of thermal expansion for unidirectional composites", *J. Compos. Mater.*, **23**, 370-381. https://doi.org/10.1177/002199838902300405
Chamis, C.C. (1984), "Simplified composite micromechanics equations of hygral, thermal, and mechanical properties", *SAMPE Quart*, **15**, 14-23.
Chattibi, F., Benrahou, K.H., Benachour, A., Nedri, K., Tounsi, A. (2015), "Thermomechanical effects on the bending of antisymmetric cross-ply composite plates using a four variable sinusoidal theory", *Steel. Compos. Struct.*, **19**(1), 93-110. http://doi.org/10.12989/scs.2015.19.1.093
Chen, J., Yang, G., Xiao, S., Chen, D., Wang, M., Jiang, L. (2024), "Effect of temperature and moisture composite environments on the mechanical properties and mechanisms of woven carbon fiber composites", *J. Polym. Compos.*, **32**, 1-18. https://doi.org/10.1002/pc.28085
Echaabi, J., Trochu, F., Pham, X.T. and Ouellet, M. (1996), "Theoretical and experimental investigation of failure and damage progression of graphite-epoxy composites in the flexural bending test", *J. Reinf. Plast. Comp.*, **15**, 740-755. https://doi.org/10.1177/073168449601500707
El Idrissi, H. and Seddouki, A. (2023), "A comprehensive study of the flexural behaviour and damage evolution of composite laminates using a progressive failure model", *Int. J. Adv. Manuf. Technol*, **127**, 3869-3890. https://doi.org/10.1007/s00170-023-11746-x
Falkowicz, K. (2023), "Experimental and numerical failure analysis of thin-walled composite plates using progressive failure analysis", *J. Compos. Struct.*, **305**, 116474. https://doi.org/10.1016/j.compstruct.2022.116474.
Greif, R. and Chapon, E. (1993), "Investigation of successive failure modes in graphite/epoxy laminated composite beams", *J. Reinf. Plast. Comp.*, **12**, 602-621. https://doi.org/10.1177/073168449301200509
Hadj-Djilani, A., Kioua, A., Zitoune, R., Toubal, L. and Bougherara, H. (2023), "Exploring the flexural and impact properties of pure flax/epoxy and Kevlar/flax/epoxy composites through experimental and numerical analysis", *Proceedings of the Institution of Mechanical Engineers*, *Part L: Journal of Materials: Design and Applications*, **237**(11), 2361-2378. https://doi.org/10.1177/14644207231178663
Hajikazemi, M. and Sadr, M.H. (2014), "Stiffness reduction of cracked general symmetric laminates using a variational approach", *Int. J. Sol. Struct.*, **51**(7-8), 1483-1493. https://doi.org/10.1016/j.ijsolstr.2013.12.040
Halpin, J.C. and Tsai, S.W. (1968), "Effects of environmental factors on composite materials", *AFML-TR*, 67-423.
Huang, Z.Q., Zhou, J.C. and Liew, K.M. (2014), "Variational analysis of angle-ply laminates with matrix cracks", *Int. J. Sol. Struct.*, **51**(21-22), 3669-3678. https://doi.org/10.1016/j.ijsolstr.2014.06.028
Katerelos, D.T.G., Krasnikovs, A. and Varna, J. (2015), "Variational models for shear modulus of symmetric and balanced laminates with cracks in 90°-layer", *Int. J. Sol. Struct.*, **71**, 169-179. https://doi.org/10.1016/j.ijsolstr.2015.06.017
Khodjet Kesba, M., Benkhedda, A., Adda Bedia, E.A. and Boukert, B. (2018), "On transverse matrix cracking in composite laminates loaded in flexure under transient hygrothermal conditions", *J. Struct. Eng. Mech.*, **67**(2), 165-173. https://doi.org/10.12989/sem.2018.67.2.165
Khodjet kesba, M., AddaBedia, E.A., Benkhedda, A. and Boukert, B. (2015), "Hygrothermal effect in [θm/90n]s cracked composite laminates-desorption case", *Procedia. Eng.*,**114,** 110-117. https://doi.org/10.1016/j.proeng.2015.08.048
Khodjet kesba, M., AddaBedia, E.A., Benkhedda, A. and Boukert B. (2016), "Prediction of Poisson's ratio degradation in hygrothermal aged and cracked $[\theta_m/90_n]_s$ composite laminates", *Steel. Compos. Struct.*, **21,** 57-72. http://doi.org/10.12989/scs.2016.21.1.057
Khodjet kesba, E.A., Benkhedda, M., AddaBedia, A. and Boukert B. (2018), "On transverse matrix cracking in composite laminates loaded in flexure under transient hygrothermal conditions", *Struct. Eng. Mech.*, **67,** 165-173. https://doi.org/10.12989/sem.2018.67.2.165
Khodjet kesba, E.A., Benkhedda, M., AddaBedia, A. and Boukert B. (2019), "Hygrothermal effect on the moisture absorption in composite laminates with transverse cracks and delamination", *Adv. Aircr. Spacecr. Sci.*,**6,** 315-331. https://doi.org/10.12989/aas.2019.6.4.315
Kumar, S., Sharma, N., Biswas, R. and Singh, K.K. (2023) "Effect of temperature on the flexural and ILSS

behaviour of symmetric and asymmetric basalt fibre-reinforced polymer composites", *Mater. Today Proc.*, In Press. https://doi.org/10.1016/j.matpr.2023.03.327.

Li, S. and Hafeez, F. (2009), "Variation-based cracked laminate analysis revisited and fundamentally extended", *Int. J. Sol. Struct.*, **46**(20), 3505-3515. https://doi.org/10.1016/j.ijsolstr.2009.03.031

Liu, Y., Wang, H., Ding, H., Wang, H. and Bi, Y. (2024), "Effect of hygrothermal aging on compression behavior of CFRP material with different layups", *J. Compos. Part B Eng.*, **270**, 111134. https://doi.org/10.1016/j.compositesb.2023.111134

Maurice, F.A. (2001), "Engineering composite materials", EMC471. The Pennsylvania, State University.

McCartney, L.N. and Pierse, C. (1997), "Stress transfer mechanics for multiple plies laminates subject to bending", *NPL Report CMMT(A)*, **55**, February.

Qiu, Z., Wu, D., Zhang, Y., Liu, C., Qian, Y. and Cai, D.A. (2024), "On the mechanical behavior of carbon fiber/epoxy laminates exposed in thermal cycling environments", *J. Thin-Wall. Struct.*, **196**, 111481. https://doi.org/10.1016/j.tws.2023.111481.

Rezoug, T., Benkhedda, A., Khodjet Kesba, M. and Addabedia, E.A. (2011), "Analysis of the composite patches cracked and aged in hygrothermal conditions", *Mech. Indus.*, **12**, 395-398. https://doi.org/10.1051/meca/2011134

Sereir, Z., Adda-Bedia, E.A. and Tounsi, A. (2006), "Effect of temperature on the hygrothermal behaviour of unidirectional laminated plates with asymmetrical environmental conditions", *Compos. Struct.*, **72**, 383-392. https://doi.org/10.1016/j.compstruct.2005.01.008

Shen, C.H. and Springer, G.S., (1981), "Moisture absorption and desorption of composite materials", *J. Compos. Mater.*, **10**(1), 2-20.

Smith, P.A. and Ogin, S.L. (1999), "On transverse matrix cracking in cross-ply laminates loaded in simple bending", *Compos. Part A*, **30**, 1003-1008. https://doi.org/10.1016/S1359-835X(99)00006-8

Smith, P.A. and Ogin, S.L. (2000), "Characterization and modelling of matrix cracking in a $(0/90)_{2s}$ GFRP laminate loaded in flexure", *Proc. R. Soc. Lond. A*, **456**, 2755-2770. https://doi.org/10.1098/rspa.2000.0638

Staab, G. (1999), *Laminar Composite*, London: Butterworth-Heinemann, U.K.

Sun, Q., Zhou, G., Tang, H., Chen, Z., Fenner, J., Meng, Z., Jain, M. and Su, X. (2021), "A combined experimental and computational analysis of failure mechanisms in open-hole cross-ply laminates under flexural loading", *J. Compos. Part B Eng.*, **215**,108803. https://doi.org/10.1016/j.compositesb.2021.108803

Tounsi, A., Adda Bedia, E.L., Benachour, A. (2005), "A new computational method for prediction of transient hygroscopic stresses during moisture desorption in laminated composite plates with different degrees of anisotropy", *Int. J. Therm. Compos. Mater.*,**18,** 37-58. https://doi.org/10.1177/0892705705041156

Tsai, S.W. (1988), *Composites Design*, Think Composites, Dayton, Paris, France.

Upadhyay, P.C. and Lyons, J.S. (2000), *Journal of Reinforced Plastics and Composites*, **19**, 465-491.

Vergnaud, J.M. (1992), *Drying of Polymeric and Solid Materials: Modelling and Industrial Applications*, Springer-Verlag, London, U.K.

Vingradov, V. and Hashin, Z. (2010), "Variational analysis of cracked angle-ply laminates", *Compos. Sci. Tech.*, **70**(4), 638-646. https://doi.org/10.1016/j.compscitech.2009.12.018

Zidi, M., Tounsi, A., Houari, M.S.A., Bedia, E.A.A. and Bég, O.A. (2014), "Bending analysis of FGM plates under hygro-thermo-mechanical loading using a four variable refined plate theory", *Aerosp. Sci. Technol.*, **34**, 24-34. https://doi.org/10.1016/j.ast.2014.02.001.

CC